

Temperature dependence of the charge carrier mobility in disordered organic semiconductors at large carrier concentrations

I. I. Fishchuk,¹ A. K. Kadashchuk,^{2,3} J. Genoe,² Mujeeb Ullah,⁴ H. Sitter,⁴ Th. B. Singh,⁵ N. S. Sariciftci,⁶ and H. Bässler⁷

¹*Institute for Nuclear Research, National Academy of Sciences of Ukraine, Prospect Nauky 47, 03680 Kyiv, Ukraine*

²*IMEC, Kapeldreef 75, Heverlee, B-3001 Leuven, Belgium*

³*Institute of Physics, National Academy of Sciences of Ukraine, Prospect Nauky 46, 03028 Kyiv, Ukraine*

⁴*Institute of Semiconductor & Solid State Physics, Johannes Kepler University of Linz, A-4040 Linz, Austria*

⁵*Molecular and Health Technologies, CSIRO, Bayview Avenue Clayton, Victoria 3168, Australia*

⁶*Linz Institute for Organic Solar Cells (LIOS), Johannes Kepler University of Linz, A-4040 Linz, Austria*

⁷*Chemistry Department, Philipps-Universität Marburg, Hans-Meerwein-Strasse, D-35032 Marburg, Germany*

(Received 18 May 2009; revised manuscript received 31 August 2009; published 8 January 2010)

Temperature-activated charge transport in disordered organic semiconductors at large carrier concentrations, especially relevant in organic field-effect transistors (OFETs), has been thoroughly considered using a recently developed analytical formalism assuming a Gaussian density-of-states (DOS) distribution and Miller-Abrahams jump rates. We demonstrate that the apparent Meyer-Neldel compensation rule (MNR) is recovered regarding the temperature dependences of the charge carrier mobility upon varying the carrier concentration but not regarding varying the width of the DOS. We show that establishment of the MNR is a characteristic signature of hopping transport in a random system with variable carrier concentration. The polaron formation was not involved to rationalize this phenomenon. The MNR effect has been studied in a OFET based on C₆₀ films, a material with negligible electron-phonon coupling, and successfully described by the present model. We show that this phenomenon is entirely due to the evolution of the occupational DOS profile upon increasing carrier concentration and this mechanism is specific to materials with Gaussian-shaped DOS. The suggested model provides compact analytical relations which can be readily used for the evaluation of important material parameters from experimentally accessible data on temperature dependence of the mobility in organic electronic devices. Experimental results on temperature-dependent charge mobility reported before for organic semiconductors by other authors can be well interpreted by using the model presented in this paper. In addition, the presented analytical formalism predicts a transition to a Mott-type charge carrier hopping regime at very low temperatures, which also manifests a MNR effect.

DOI: [10.1103/PhysRevB.81.045202](https://doi.org/10.1103/PhysRevB.81.045202)

PACS number(s): 72.20.Jv, 72.20.Ee, 72.80.Le, 72.80.Ng

I. INTRODUCTION

Many modern electronic solid-state devices such as organic field-effect transistors (OFETs), organic light-emitting diodes (OLEDs) and solar cells, or electrophotographic photoreceptors employed in today's photocopiers, are generally based upon noncrystalline materials such as organic semiconductors¹⁻³ or amorphous silicon. In order to improve their operation, it is essential to understand how charge carriers in amorphous solids are transported. In crystalline materials, electronic transport in delocalized band states exists. In contrast, the random structure present in amorphous solids implies that the electronic states are localized and energetically distributed, so that transport occurs via incoherent hopping⁴⁻⁶ in this density of states (DOS). During device operation, only part of the DOS is populated by charges. The shape of the DOS and its occupied fraction determine the transport properties of the material. There are two limiting cases. (i) An amorphous solid is intrinsically an insulator, as is the case for many organic π -conjugated materials. Their electronic transport is due to extrinsic charges that are either injected from the electrodes or that are created by photogeneration or chemical doping. In these materials, the density of occupied transport states (n) is much lower than the total density of states (N), i.e., $n \ll N$. Therefore, each charge carrier explores an essentially empty DOS. If the DOS is a

Gaussian with variance σ , the (almost infinitely diluted) ensemble of noninteracting carriers at not too low temperatures has been shown to form an occupational density-of-states distribution (ODOS) (Ref. 4) of the same Gaussian shape yet displaced by an energy $\varepsilon_0 = -\sigma^2/k_B T$ below the center of the DOS. The latter is the energy at which, on average, charge carriers migrating within a Gaussian DOS distribution settle in the limit of very weak carrier density.⁴ In this case the Fermi level ε_F is far below the thermal quasiequilibrium level ε_0 and, as a consequence, is irrelevant for charge hopping process. Charge transport requires jumps from temporarily filled ODOS states to empty DOS states and the temperature dependence of the charge mobility follows $\ln(\mu) \propto T^{-2}$ law^{4,6} and does not depend on carrier concentration. (ii) The other extreme is realized in low band-gap disordered inorganic semiconductors, such as amorphous silicon. In this case part of the DOS is filled so that a Fermi level is established and Fermi-Dirac distribution determines the ODOS. Here, for *not too low temperatures*, the charge carrier mobility features a simple thermal activation dependence $\ln(\mu) \propto T^{-1}$ with virtually constant activation energy reflecting the temperature-independent position of the Fermi level ε_F with respect to the mobility edge,⁷ although the activation energy does depend on charge carrier concentration reflecting the concentration shift of the Fermi level. At very low temperatures, charge transport in these materials occurs via Mott

variable-range hopping (VRH) near the Fermi level featuring a $\ln(\mu) \propto T^{-1/4}$ law.⁸

An intermediate situation is established when in an intrinsically insulating material a sizeable fraction of available hopping states are occupied. This is realized, for example, in an OFET in which transport is confined to a very thin transport channel so that the relative carrier concentration (n/N) can reach values of 10^{-2} or higher.⁹ Measurements of the charge carrier mobility in organic materials at large carrier concentrations and moderately large temperatures have revealed an Arrhenius-type $\ln(\mu) \propto T^{-1}$ dependence that extrapolates to an unusually high prefactor mobility of 30–40 $\text{cm}^2/\text{V s}$ (Ref. 10) which exceeds values determined via time-of-flight (ToF) technique by 2–3 orders of magnitude.^{4,6} Interestingly, Arrhenius-type $\mu(T)$ dependences, measured at different gate voltage and, concomitantly, the charge carrier densities, and on different OFET structures intersect at a given finite T_0 , suggesting that the Meyer-Neldel rule (MNR) (Ref. 11) is obeyed.

The MNR is an empirical relation, originally derived from chemical kinetics.¹¹ It describes the fact that enthalpy and entropy of a chemical reaction are proportional. More generally, it states that in a thermally activated rate process an increase in the activation energy E_a is partially compensated by an increase in the prefactor so that

$$R(T) = R_0 \exp\left(\frac{E_a}{E_{\text{MN}}}\right) \exp\left(-\frac{E_a}{k_B T}\right), \quad (1)$$

where E_{MN} is called the "Meyer-Neldel energy." There are numerous examples, notably, in semiconductor physics in which the MNR is fulfilled. In context of multiple trapping dominated charge transport it was associated with the presence of the exponential distribution of traps.^{12–16} Widenhorn *et al.*¹⁷ argue that the MNR arises for an arbitrary system where an intrinsic rate process as well as an impurity related process both contributes while Yelon and Movaghar¹⁸ suggest that the MNR is obeyed when a thermally activated process requires a large number of individual excitations which increase the entropy. Recently, Emin¹⁹ advanced an adiabatic polaron hopping model that considers carrier-induced softening of the vibrations upon electron motion and showed that this brings up the MNR. This model, however, neglects energetic disorder; though superimposition of polaron and disorder effects was shown to be important in some amorphous organic materials.^{6,20}

In the present work, we have applied the recently suggested theory based upon the "effective medium approximation" (EMA),²¹ which is based on a Gaussian DOS distribution and Miller-Abrahams jump rates. We have considered thoroughly the temperature dependence of the charge mobility in disordered organic solids at large carrier concentrations. In particular, we aimed to rationalize the physics behind the experimentally observed MNR effect and related phenomena in the framework of a hopping-transport model with accounting for the evolution of the occupied DOS distribution as a function of carrier concentration in a Gaussian-type inherent disordered system. We shall show that the establishment of the MNR is a characteristic signature of hopping transport in a random system with variable carrier

concentration irrespective of their polaronic character. The present theory was applied to describe the observed MNR behavior for the OFET mobility at moderately high temperatures in C_{60} films thermally evaporated at room temperature. This experiment provides unambiguous test for the suggested model because energetic disorder effects are expected to dominate the thermally activated transport in C_{60} owing to the smallest electron-phonon coupling in this material²² among other aromatic molecular systems, that is also supported by the almost temperature-independent charge mobility in C_{60} single crystals.²³ We show that the MNR effect for the OFET mobility experimentally observed before for other organic semiconductors can also be well interpreted by the present theory. Besides, for completeness sake, the suggested theoretical formalism was also extended down to very low temperatures and a Mott-type charge carrier hopping regime has been reproduced in such case.

II. THEORETICAL CONSIDERATION

We consider a disordered organic semiconductor containing localized sites with an average intersite distance $a = N^{-1/3}$, where N is the concentration of the localized states, and a charge carrier transport in such a material, which occurs by thermally assisted hopping. The present model is based solely on disorder formalism and we restrict our consideration here by single-phonon hopping processes through the manifold of localized sites, i.e., any polaron effects are ignored. Assuming that in the relevant organic optoelectronic materials, e.g., C_{60} , polythiophene-type conjugated polymers, etc., electron-phonon coupling is weak enough with respect to energetic disorder (note that polaron contribution to the activation transport is only one quarter of the reorganization energy) and, consequently, charge transport is controlled by disorder,^{4–6} we use Miller-Abrahams-type jump rate $W_{ij} = \nu_0 \exp(-2r_{ij}/b) \exp\{-[|\varepsilon_j - \varepsilon_i| + (\varepsilon_j - \varepsilon_i)]/2k_B T\}$ for an elementary charge transfer between sites with energy ε_j and ε_i with the intersite distance r_{ij} , and the concept of the effective transport energy.⁶ In our model we use (unless otherwise specified) a Gaussian DOS distribution. The essential system parameters are the variance σ of the Gaussian DOS, $g(\varepsilon) = (N/\sigma\sqrt{2\pi}) \exp[-(1/2)(\varepsilon/\sigma)^2]$, the ratio of densities of occupied and total transport states n/N , and the ratio a/b of the intersite distance (a) and the localization radius (b) of the charged site. For arbitrary charge concentration the normalized ODOS distribution is given by

$$P(\varepsilon) = \frac{g(\varepsilon)f(\varepsilon, \varepsilon_F)}{\int_{-\infty}^{\infty} d\varepsilon g(\varepsilon)f(\varepsilon, \varepsilon_F)}, \quad (2)$$

where $f(\varepsilon, \varepsilon_F)$ is given by the Fermi-Dirac statistics and ε_F is the Fermi level obtained from $n = \int_{-\infty}^{\infty} d\varepsilon g(\varepsilon)f(\varepsilon, \varepsilon_F)$.

Effective hopping charge mobility in disordered organic solids can be obtained via calculation of the effective jump rate W_e of the intersite transition within the Miller-Abrahams model at arbitrary relative concentration, n/N , of charge carriers. Such calculations have been done recently by the EMA method using the concept of effective transport energy, ε_p ,²¹

and the result for the effective mobility μ_e reads

$$\mu_e = \mu_0 x k_0 \left(\frac{r_t}{a}\right)^2 \exp\left(-2\frac{r_t}{b}\right) \exp\left(-xx_t\right) \frac{\int_{-\infty}^{x_t} dt \frac{\exp\left(-\frac{1}{2}t^2 + xt\right)}{1 + \exp[x(t-x_F)]}}{\int_{-\infty}^{x_t} dt \frac{\exp\left(-\frac{1}{2}t^2\right)}{1 + \exp[x(t-x_F)]}}, \quad (3)$$

where b is the localization radius of a charge carrier (it is assumed that $b \ll a$), $\mu_0 = ea^2\nu_0/\sigma$, ν_0 is the attempt-to-escape frequency, $x = \sigma/k_B T$, $x_t = \varepsilon_t/\sigma$, $x_F = \varepsilon_F/\sigma$, and

$$r_t = a \left[\frac{4\pi}{3} \frac{1}{\sqrt{2\pi}} \int_{-\infty}^{x_t} dt \frac{\exp\left(-\frac{1}{2}t^2\right)}{1 + \exp[-x(t-x_F)]} \right]^{-1/3}, \quad (4)$$

$$\frac{1}{\sqrt{2\pi}} \frac{\exp\left(-\frac{1}{2}x_t^2\right)}{1 + \exp[-x(x_t-x_F)]} \left[\frac{1}{\sqrt{2\pi}} \int_{-\infty}^{x_t} dt \frac{\exp\left(-\frac{1}{2}t^2\right)}{1 + \exp[-x(t-x_F)]} \right]^{-4/3} = \frac{3}{2} \left(\frac{4\pi}{3}\right)^{1/3} \frac{b}{x a}. \quad (6)$$

It should be noted that the effective transport energy concept is justified at a considerable degree of the energetic disorder, i.e., the Eq. (6) is valid only at $\sigma/k_B T > 1$.

A. High-temperature region

Figure 1(a) (bold curves) shows the calculated temperature dependences of the effective mobility, plotted in a $\ln(\mu_e/\mu_0)$ vs $\sigma/k_B T$ representation for different charge carrier concentrations assuming $a/b=10$. The calculations are restricted to a temperature regime defined by $\sigma/k_B T \geq 3$. The Arrhenius type of the $\mu(T)$ dependence indicates that the ODOS is virtually temperature independent. This is quite in contrast of the case of $n/N \rightarrow 0$ characterized by the non-Arrhenius-type temperature dependence $\ln(\mu_e/\mu_0) \propto (\sigma/k_B T)^2$ since in such a case charge transport is dominated by the hopping from the equilibrium occupational DOS distribution which is temperature dependent.

A remarkable result is that if one would—hypothetically—extend the above calculations to higher temperatures the asymptotes (thin lines) would intersect at finite temperature $T_0 \cong 2\sigma/5k_B$. Note that the EMA (Ref. 21) does not allow presenting the results in closed analytic form. However, the calculated results including their (hypothetical) extension toward infinite T can be parameterized in terms of an approximate analytical equation for the charge carrier mobility μ_e as a function of $\sigma/k_B T$, a/b , and n/N ,

$$k_0 = 1 - \frac{\int_{-\infty}^{\infty} dt \frac{\exp\left(-\frac{1}{2}t^2\right)}{\{1 + \exp[x(t-x_F)]\}^2}}{\int_{-\infty}^{\infty} dt \frac{\exp\left(-\frac{1}{2}t^2\right)}{1 + \exp[x(t-x_F)]}}. \quad (5)$$

Parameter k_0 appears in Eq. (3) due to employment of the generalized Einstein equation as recently suggested by Roichman and Tessler,²⁴ relating the mobility and diffusion coefficient. This coefficient is essential at large carrier concentrations, while in the case of $n/N \rightarrow 0$, Eq. (5) yields $k_0 \rightarrow 1$. The effective transport energy ε_t is defined as the energy of a target site to which most of localized carriers make thermally activated jumps with a jump rate independent on the energy of a starting state and it can be determined from the following transcendental equation

$$\mu_e = \mu_0 \exp\left[-2\frac{a}{b} + \frac{1}{2}\left(\frac{a}{b} - 7\right)\right] \exp\left\{-\left[\frac{3}{40b} - \frac{1}{15b} \log_{10}\left(\frac{n}{N}\right)\right] \left(\frac{\sigma}{k_B T} - y_0\right)\right\}, \quad (7)$$

where $y_0 = 21/10 + (1/25)(a/b)$. It is appropriate for $8 < a/b < 12$ and for $10^{-3} \leq n/N \leq 10^{-1}$ which is a relevant set of parameters to describe OFET operation. The inset in Fig. 1(a) proves that the isokinetic temperature T_0 , at which the $\ln(\mu_e) \propto T^{-1}$ graphs intersect, depends rather weakly on a/b . Rewriting Eq. (7) yields

$$\mu_e = \mu_0 \exp\left[-2\frac{a}{b} + \frac{1}{2}\left(\frac{a}{b} - 7\right)\right] \exp\left[-E_a \left(\frac{1}{k_B T} - \frac{1}{k_B T_0}\right)\right], \quad (8)$$

where

$$E_a = \left[\frac{3}{40b} - \frac{1}{15b} \log_{10}\left(\frac{n}{N}\right)\right] \sigma, \quad T_0 = \frac{E_{MN}}{k_B} = \frac{\sigma}{k_B y_0}. \quad (9)$$

It turns out that Eq. (8) can be extended to lower carrier concentrations, $10^{-5} \leq n/N < 10^{-3}$, (relevant for an OLED operation), if E_a is substituted by $E'_a = 0.85E_a$.

As one can note, Eq. (8) is nothing else than the conventional Meyer-Neldel-type relation [cf. Eq. (1)] that has been verified by experiments on several OFET devices.²⁵⁻²⁷ A certain compensation effect is evident from Eq. (8) that is the

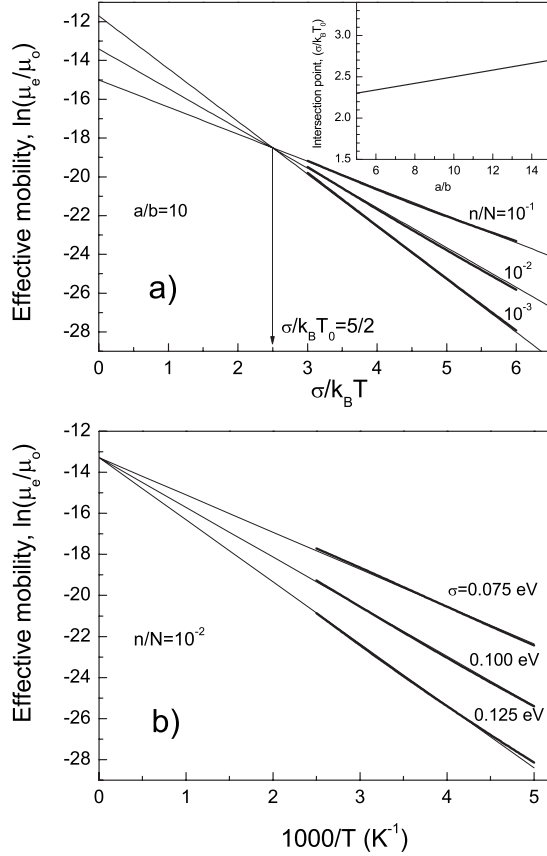


FIG. 1. (a) Dependence of effective charge carrier mobility $\ln(\mu_e/\mu_0)$ on $\sigma/k_B T$ at different effective carrier concentrations calculated by Eqs. (2)–(6) (bold curves) at $\sigma/k_B T \geq 3$ and $a/b=10$. The inset shows the intersection point $\sigma/k_B T_0$ vs a/b ratio. (b) $\ln(\mu_e/\mu_0)$ vs $1/T$ dependences at different width of the DOS, σ , calculated by Eqs. (2)–(6) (bold curves) at constant carrier concentration $n/N=10^{-2}$ and $a/b=10$. Thin lines represent the approximated dependences calculated by Eq. (8).

essence of the Meyer-Neldel compensation rule. Note, that the prefactor of mobility is a product of parameter μ_0 and the temperature-independent exponential term in Eq. (8). Let us rewrite Eq. (8) as

$$\mu_e = \mu_{00} \exp\left(-\frac{E_a}{k_B T}\right), \quad (10)$$

where

$$\mu_{00} = \mu_0 \exp\left[-2\frac{a}{b} + \frac{1}{2}\left(\frac{a}{b} - 7\right) + \frac{E_a}{k_B T_0}\right]. \quad (11)$$

Then one can obtain

$$\ln\left(\frac{\mu_{00}}{\mu_0}\right) = -2\frac{a}{b} + \frac{1}{2}\left(\frac{a}{b} - 7\right) + \frac{E_a}{k_B T_0}. \quad (12)$$

Equation (12) relates the prefactor μ_{00} with the activation energy E_a , namely, predicts a linear relationship between $\ln \mu_{00}$ and E_a , which was often observed in experiments.

If one assumes $\sigma=0.1$ eV and $a/b=10$, a typical value for organic disordered materials, a Meyer-Neldel energy $E_{MN}=k_B T_0=0.04$ eV is obtained, a value which indeed has been typically observed in many relevant experiments. The activation energy E_a [Eq. (9)] is temperature independent and varies linearly with σ —decreases with increasing charge carrier concentration due to the shift of the Fermi level^{21,25} toward the effective transport energy level. We should emphasize on an important consequence of the presented theoretical model that it provides compact analytical relations [viz. Eqs. (8) and (9)] which can be readily used for the estimation of important material parameters and effective carrier concentration from experimentally accessible data on temperature dependence of the mobility measured in organic semiconductor-based devices. The width of the DOS $\sigma=5E_{MN}/2$ can be obtained from experimentally determined quantity E_{MN} assuming a typical value $a/b=10$. Equation (9) yields an estimate for the effective carrier concentration n/N from the experimentally measured E_a .

Interestingly, the structure of Eq. (8) predicts that if one extends a family of $\ln(\mu_e)$ vs T^{-1} graphs calculated at variable E_a , i.e., by changing the active organic semiconductor layer, yet constant carrier concentration, to $T \rightarrow \infty$ they would intersect at infinite temperature rather than at finite T_0 as MNR would imply. Figure 1(b) shows temperature dependences of the effective mobility calculated by Eqs. (2)–(6) (bold lines) and approximated Eq. (8) (thin lines) for different energetic disorder parameter σ , yet constant carrier concentration $n/N=10^{-2}$ and $a/b=10$. The calculations presented in Fig. 1 are restricted to a temperature range of moderately high temperatures. As it is evident from Fig. 1(b), the calculated temperature dependences in this case *do not show* any MNR compensation effect and intersect at the infinite temperature. This is in disagreement with the conventional MNR that predicts a correlation between prefactor rate and activation energy regardless of how the change in E_a is accomplished, i.e., by either changing the width of the DOS itself or changing the degree of state filling.

B. Low-temperature region

The results presented in the preceding section cover a range of not too low temperatures, i.e., when $\sigma/k_B T \leq 6$, and an Arrhenius-type temperature dependence of the charge mobility $\ln \mu_e \propto 1/T$ was recovered for high carrier densities (Fig. 1). Hence, Eq. (7) is applicable until *moderately low* temperatures only, when thermally activated jumps occur to the effective transport energy level which is rather close to the DOS center. Upon going to very low temperature, the calculated temperature dependences of charge mobility [using Eqs. (2)–(6)] are found to become progressively weaker as shown in Fig. 2 (bold curves), so they no longer could be extrapolated by Eq. (7) (thin curves).

The reason for such a behavior is the following. The effective transport energy level ε_t is a temperature-dependent quantity [cf. Eq. (6)] (this conclusion is also supported by previous studies^{28–30}) and it shifts toward deeper tail states of the DOS distribution with further lowering temperature,²¹ so it eventually approaches the Fermi level ε_F which features a

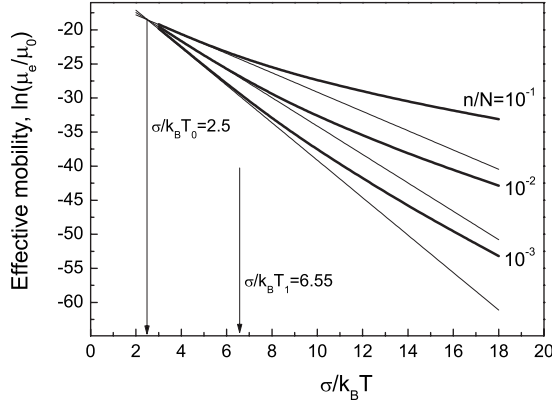


FIG. 2. Dependence of effective charge carrier mobility $\ln(\mu_e/\mu_0)$ on $\sigma/k_B T$ calculated until very low temperatures by Eqs. (2)–(6) (bold curves) at different carrier concentrations at $a/b=10$. Extrapolation of the high-temperature branch of the charge mobility by Eq. (7) is shown by thin curves.

much-flattened temperature dependence. This is depicted in the Fig. 3 where the effective transport energy level ε_t (solid curves) and Fermi level ε_F (dashed curves) are plotted as a function of temperature for two different carrier concentrations $n/N=10^{-1}$ and 10^{-4} . Thus, at sufficiently low temperatures one might expect an establishment of a charge transport regime resembling a Mott-type VRH $\ln \mu_e \propto (1/T)^{1/4}$.

Figure 4 shows temperature dependences of the effective mobility calculated by Eqs. (2)–(6) (bold curves) for different charge carrier concentrations at very low temperatures when $(\sigma/k_B T)^{1/4} \gg 1$ and plotted in Mott representation as $\ln(\mu_e/\mu_0)$ vs $(\sigma/k_B T)^{1/4}$. From Fig. 4 it is evident that the calculated temperature dependences are straight lines in Mott representation bearing out an establishment of a Mott-type hopping transport. This result is in accord with recent calculations³¹ predicted a crossover of different hopping conduction regimes in the same organic material, namely, “activation to the transport level” and “Mott-type VRH,” depending on carrier density and temperature. Similar reason for the breaking down the $1/T$ dependence of $\log(\mu_{eff})$ at low tem-

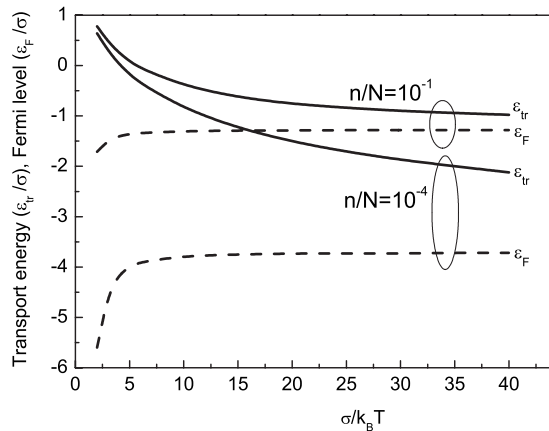


FIG. 3. Temperature dependence of the effective transport energy level ε_t (solid curves) and Fermi level ε_F (dashed curves) calculated at different carrier concentrations $n/N=10^{-1}$ and 10^{-4} indicated in the figure.

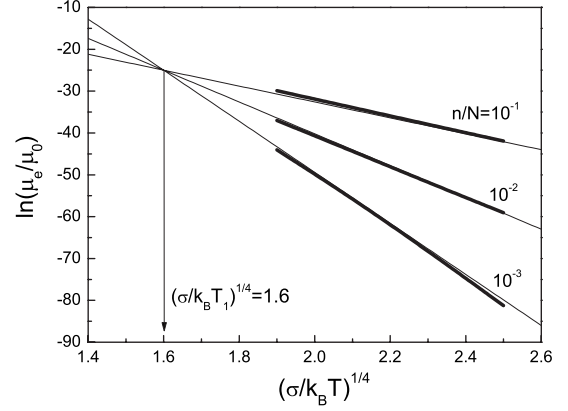


FIG. 4. Dependence of the effective charge carrier mobility $\ln(\mu_e/\mu_0)$ versus $(\sigma/k_B T)^{1/4}$ at different carrier concentrations calculated by Eqs. (2)–(6) (bold curves) for low-temperature region at $(\sigma/k_B T)^{1/4} \gg 1$ and assuming $a/b=10$. Thin lines present the approximation dependences calculated by Eq. (17).

peratures in an organic material was suggested also by Coehoorn and co-workers^{32,33} employing numerical simulations by the master-equation approach.

Interestingly, that asymptotes of the calculated dependences (thin lines) are found to intersect at some intermediate (finite) temperature $T_1 = \sigma/(1.6)^4 k_B$ resembling a NMR behavior. We found that the calculation results on the temperature dependences of the effective mobility μ_e (Fig. 4) can be well approximated at $a/b=10$ by the following expression (thin lines)

$$\mu_e = \mu_0 \exp \left[-2 \frac{a}{b} + \frac{1}{2} \left(\frac{a}{b} - 20 \right) \right] \exp \left\{ -Y_a \left[\left(\frac{\sigma}{k_B T} \right)^{1/4} - y_1 \right] \right\}. \quad (13)$$

where

$$Y_a = -2 \left[1 + \frac{a}{b} \log_{10} \left(\frac{n}{N} \right) \right], \quad y_1 = \frac{1}{2} \left(3 + \frac{1}{50} \frac{a}{b} \right). \quad (14)$$

Let us rewrite Eq. (13) in the following form

$$\mu_e = \mu_0 \exp \left[-2 \frac{a}{b} + \frac{1}{2} \left(\frac{a}{b} - 20 \right) \right] \exp \left\{ -Y_a \left[\left(\frac{\sigma}{k_B T} \right)^{1/4} - \left(\frac{\sigma}{k_B T_1} \right)^{1/4} \right] \right\}, \quad (15)$$

where

$$T_1 = \frac{\sigma}{k_B Y_1^4}. \quad (16)$$

Equation (15) can be further rewritten in a conventional “MNR form”

$$\mu_e = \mu_0 \exp \left[-2\frac{a}{b} + \frac{1}{2} \left(\frac{a}{b} - 20 \right) \right] \exp \left\{ - \left[\left(\frac{T_a}{T} \right)^{1/4} - \left(\frac{T_a}{T_1} \right)^{1/4} \right] \right\}, \quad (17)$$

where $T_a = Y_a^4 \sigma / k_B$. Analysis shows that the approximated Eq. (17) can be well used for approximations of the calculated $\mu_e(T)$ for the high carrier density ranging within $10^{-3} < n/N < 10^{-1}$ when $8 < a/b < 12$. If one assumes $\sigma = 0.088$ eV, then one obtains $T_0 = 408$ K [for the high-temperature branch of $\mu_e(T)$] and $T_1 = 156$ K (for low-temperature branch plotted in Mott representation). Experimentally accessible parameter T_1 allows evaluation of σ and the carrier concentration n/N can be estimated from T_a . Within the presented model, σ and n/N should be the same for both Mott-type (low-temperature) and Arrhenius-type (high-temperature) regimes. Note, that both regimes follow from the same EMA theory.

Let us rewrite Eq. (17) as

$$\mu_e = \mu_{00} \exp \left[- \left(\frac{T_a}{T} \right)^{1/4} \right], \quad (18)$$

where

$$\mu_{00} = \mu_0 \exp \left[-2\frac{a}{b} + \frac{1}{2} \left(\frac{a}{b} - 20 \right) + \left(\frac{T_a}{T_1} \right)^{1/4} \right]. \quad (19)$$

Then one can obtain

$$\ln \left(\frac{\mu_{00}}{\mu_0} \right) = -2\frac{a}{b} + \frac{1}{2} \left(\frac{a}{b} - 20 \right) + \left(\frac{T_a}{T_1} \right)^{1/4}. \quad (20)$$

Equation (20) relates the prefactor μ_{00} with the activation temperature T_a , namely, $\ln \mu_{00} \propto T_a^{1/4}$. It worth noting that the obtained Eq. (20) is in agreement to the corresponding relation between the prefactor conductivity σ^{00} and the activation temperature T_0 in the equation for conductivity $\sigma = \sigma^{00} \exp[-(T_0/T)^{1/4}]$ obtained recently by numerical calculations by Godet³⁴ for exponential DOS, and which found out that $\ln \sigma^{00} \propto T_0^{1/4}$.

III. EXPERIMENTAL

The bottom gate-top contact OFET devices based on C₆₀ films were fabricated using divinyltetramethyldisiloxane-bis(benzocyclobutane) as gate-insulating layer. The thin film of C₆₀ was deposited by means of thermal evaporation at room temperature using a Leybold Univex system at a base pressure of 1×10^{-6} mbar. These films were polycrystalline in nature. Finally LiF/Al top contacts were evaporated in high vacuum. The reason to choose the top contact geometry in the present experiment is because of lower contact resistance of this geometry in comparison to the bottom contact geometry. The completed devices were loaded for electrical characterization in an Oxford cryostat under nitrogen atmosphere inside the glove box to avoid an exposure to ambient condition. All measurements were carried out at a vacuum of around 10^{-6} mbar and the temperature was changed in the range from 300 to 77 K. The measurements were conducted

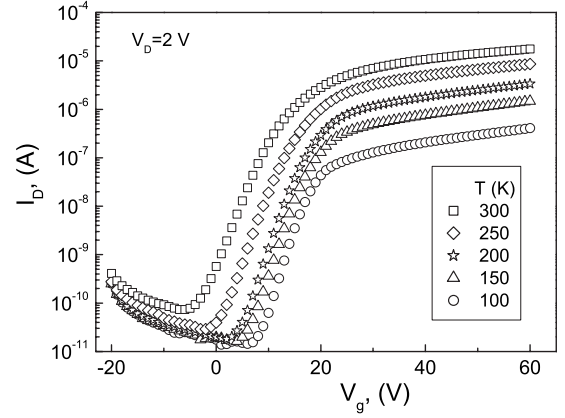


FIG. 5. Transfer characteristics of the C₆₀-based OFET at $V_D = 2$ V measured at various temperatures from 300 to 100 K. The device channel width was $W = 2$ mm and the channel length $L = 35$ μm with a capacitance of the insulator per unit area of 1.2×10^{-9} nF/cm².

with a temperature step of 10 K. Between every temperature step there was a time delay of 1 h so that the device got thermally stabilized. The transistor characteristics were recorded by Agilent 2000 SMU.

IV. EXPERIMENTAL RESULTS

The field-effect mobility μ_{FE} of the C₆₀-based organic field-effect transistors (OFET) has been determined in the linear regime of the I_D - V_g characteristics (at low source-drain voltage $V_D = 2$ V) shown in Fig. 5. The applied source-gate electric field in this regime was much larger than the in-plane source-drain field, which resulted in an approximately uniform density of charge carriers in the conductive channel.

Figure 6(a) (symbols) shows the field-effect mobility μ_{FE} as a function of inverse temperature measured for moderately large temperatures in the C₆₀ OFETs at different gate voltages V_g . It is evident that the extrapolation of these $[\ln(\mu_{FE}) \text{ vs } T^{-1}]$ graphs intersect at the isothermal temperature $T_0 = 408$ K, thus clearly demonstrating a MNR-type behavior. This yields a corresponding MNR energy of $E_{MN} = 34$ meV, which is similar to the value of 36 meV reported before for C₆₀.^{14,27} Figure 6(b) shows exactly what MNR formally predicts, namely, that the prefactor μ_{00} depends linearly on the activation energy E_a on an exponential scale and can be well fitted with Eq. (11).

It should be noted, at temperatures below ~ 160 – 170 K the above temperature dependences get considerably weaker suggesting a different transport regime at such low temperatures. This experimentally observed weak temperature dependence of mobility is qualitatively similar to the effect of weakening $\mu_e(T)$ dependences at very low temperatures shown in Fig. 2 and discussed in Sec. II B. However, this issue is beyond the scope of the present study and proper quantitative description of the low-temperature experimental data requires further advancing the current version of the EMA theory.

The experimental data on the OFET mobility in C₆₀ films at moderately large temperatures can be successfully fitted

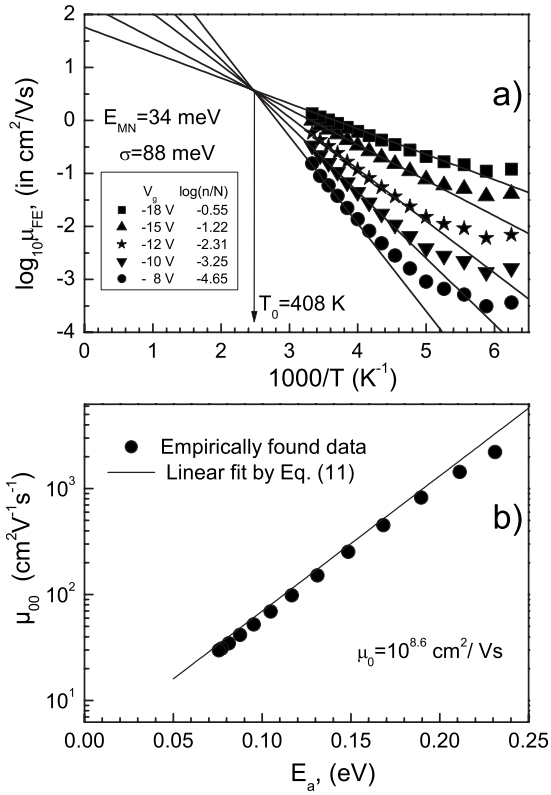


FIG. 6. (a) Temperature dependence of the OFET mobility in C₆₀ films measured at different V_g (symbols) and results of their fitting with Eq. (8) (solid lines). The isothermal temperature T_0 is indicated by an arrow. The width of the DOS (σ) and the effective carrier concentrations $\log_{10}(n/N)$ for the corresponding V_g are shown in the inset. (b) Experimentally determined data (symbols), plotted versus the activation energy determined from Fig. 6(a) and results of their fitting by Eq. (11) (solid line).

with Eq. (8) [solid curves in Fig. 6(a)]. The disorder parameter $\sigma = 0.088$ eV has been evaluated from the obtained isothermal temperature T_0 using Eq. (9) and assuming a typical value $a/b = 10$ for organic materials. The experimentally assessable activation energies for the OFET mobility measured at different gate voltages V_g allowed to calculate the effective carrier concentrations in the conductive channel of this OFET (listed in the inset), which strongly increases with increasing V_g . The fact that for $T < T_0$ the activation energy E_a [Eq. (9)] decreases at increasing gate voltage is an indication that the ODOS shifts closer to the center of DOS upon increasing n/N . The obtained σ value is a typical value for a disordered organic material derived from time-of-flight studies for charge transport.⁴ Note, however, that the experimental data cover only the $T < T_0$ regime, i.e., there is no experimental proof that the extrapolation on $\mu(T)$ toward $T > T_0$ is justified. In fact, we shall argue that this extrapolation is principally unwarranted.

In order to verify the applicability of the suggested model, it was also used to describe a few other relevant results for different organic semiconductors obtained before.^{25,26} As an example the data for the hole mobility in a small-molecule solution-processed pentacene OFET (Ref. 25) are shown in

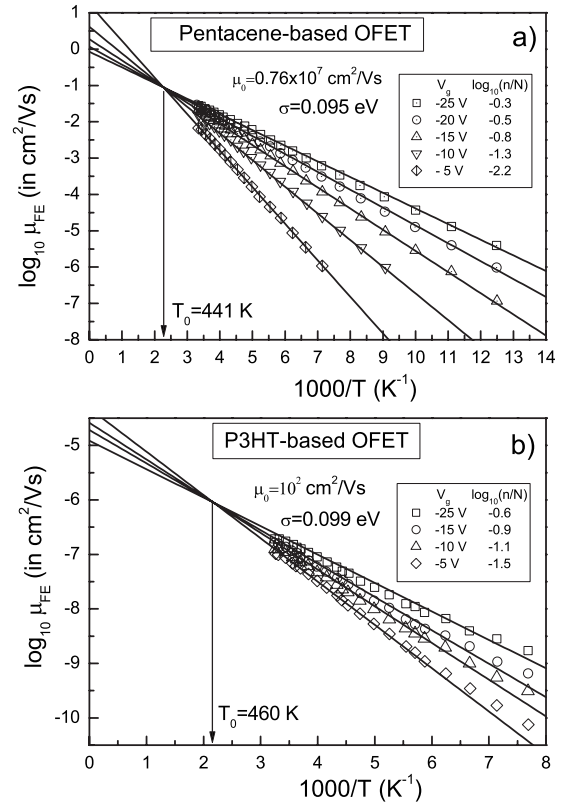


FIG. 7. Temperature dependence of the OFET mobility in solution-processed (a) pentacene and (b) P3HT measured at different V_g (symbols) (Refs. 25 and 26) and results of their fitting with Eq. (8) (solid lines) assuming $a/b = 10$. MNR isothermal temperature is indicated by arrow. Estimated disorder parameters, parameter μ_0 in Eq. (8) and the effective carrier concentrations $\log_{10}(n/N)$ for corresponding gate voltages are shown in the figure.

Fig. 7(a) (symbols). Assuming $a/b = 10$, the fit with Eq. (8) [straight lines in Fig. 7(a)] translates the observed isokinetic temperature $T_0 = 441$ K into $\sigma = 0.095$ eV. The estimated effective carrier densities in the conductive channel at different V_g are listed in the inset.

Another example is the temperature dependence of the hole mobility in poly-3-hexylthiophene (P3HT) OFETs.²⁶ The data (symbols) and the fitting by Eq. (8) (solid lines) are shown in Fig. 7(b). The results bear a typical MNR behavior with an isokinetic temperature $T_0 = 460$ K that translates into $\sigma = 0.099$ eV. This is in excellent agreement with the value of 0.098 eV derived before for this material.³⁵ A rather similar disorder parameter ($\sigma = 0.11$ eV) we found before²¹ by fitting the concentration dependence of the charge carrier mobility in P3HT.³⁵ Thus, both carrier concentration and temperature dependence of the OFET mobility can be consistently described in the framework of the same EMA theory.

V. DISCUSSION

A. Temperature dependence of the mobility: Carrier concentration vs energetic disorder effect

As described above, the presented theoretical model premised a Gaussian DOS distribution and rigid matrix approxi-

mation (Miller-Abrahams jump rate) and ignores polaronic effect. It predicts a MNR-type temperature dependence for the OFET mobility *upon varying carrier concentration* [Fig. 1(a)]. This model is an alternative to the polaron-based model developed by Emin¹⁹ to explain the MNR phenomenon in organic semiconductors devoid of energetic disorder. It worth noting that a model based on Fröhlich surface polaron³⁶ was recently suggested to rationalize strong influence of polar gate dielectrics on charge mobility in OFETs.³⁷ The Fröhlich surface polaron might be formed due to strong coupling of a charge carrier at the interface to an ionic polarization cloud of sufficiently polar gate dielectric (high-permittivity dielectric) even in organic materials with moderate or weak electron-phonon coupling.³⁷ Although this model looks interesting and is worth further development, for instance, by accounting also for some disorder effects, its consideration is beyond the scope of the present study. Moreover, we used just a nonpolar organic gate dielectric for fabrication of the C₆₀-based OFETs, so formation of the Fröhlich surface polaron is unlikely in this case. The present study demonstrates that the MNR behavior can be successfully rationalized also in the framework of a conventional hopping-transport approach based solely on disorder arguments without necessity to invoke polaron formation. We showed that the present model provides a link between the isokinetic temperature T_0 and the width of the Gaussian DOS, σ [Eq. (9)]. Finally, we want to emphasize that our approach does not exclude at all the polaron formation in organic solids; the polaron effects might be readily incorporated into the present Gaussian disorder model via employing the Marcus jump rate and the MNR behavior retains (to be presented elsewhere).

An important experimental verification of the suggested theory is that the MNR behavior is clearly observed for the OFET mobility in C₆₀ films [Fig. 6(a)] as in this material the disorder effects dominate charge transport. This is due to the smallest electron-phonon coupling in this material²² among other aromatic molecular systems, which is shown to be inversely proportional to the number of π -bonded atoms.²² Indeed, in contrast to C₆₀ films deposited by thermal evaporation, C₆₀ single crystals are normally characterized by almost temperature-independent mobility,²³ whereas small polaron motion (Holstein polaron model) requires an activation energy equal to the half of the polaron binding energy. On the other hand, thermal activation of the mobility has been measured in deposited C₆₀ films in the OFET configuration (in which a Fermi level is established) as evidenced from Fig. 6(a). The temperature dependence of the mobility arises evidently due to the disordered nature of the thin C₆₀ films as compared to single-crystal counterparts and this justifies a key role of the energetic disorder on charge mobility in this material. As one can see from the fit in Fig. 6(a) (solid curves) the present theory describes successfully the data on $\mu(T)$ dependence of the OFET mobility in C₆₀ films upon different gate voltage and the observed isokinetic temperature $T_0=408$ K yields the energetic disorder parameter $\sigma=0.088$ eV for these films. The similar MNR-type behavior observed before for small-molecule- and polymer-based OFETs, namely, pentacene- and P3HT-based OFETs (Refs. 25 and 26) can also be perfectly described by the present

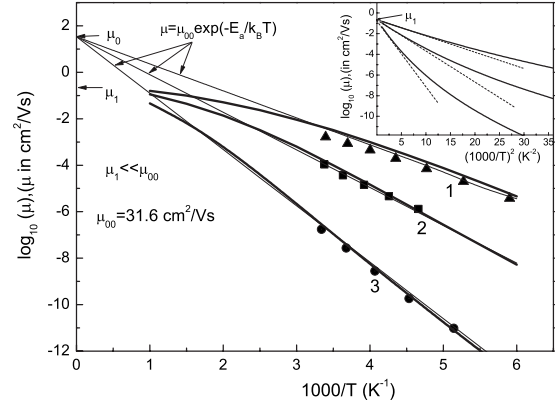


FIG. 8. Temperature dependence for the charge mobility measured in (1) PCBM, (2) region-regular P3HT, and (3) OC₁C₁₁-PPV (symbols) (Ref. 10). Extrapolation by Eq. (8) of the data to $T \rightarrow \infty$ are given by thin curves. Fitting the experimental data by Eqs. (2)–(6) is shown as bold curves. The effective carrier concentration was $n/N=1.4 \times 10^{-5}$. The inset shows the same calculated dependences plotted in $\log_{10}(\mu_e) \propto T^{-2}$ representation that yields the $T \rightarrow \infty$ intercept μ_1 .

theory [Figs. 7(a) and 7(b)] and provides an estimate of σ values for these materials, which are in agreement with the parameters determined before for these systems.

A remarkable finding is that *varying the energetic disorder*, however, *does not show* the MNR effect in disordered organic semiconductors. We want to stress that this theoretical prediction also agrees with experimental observations. Figure 8 (symbols) presents fitting of the experimental $\ln(\mu) \propto T^{-1}$ data from Ref. 10 taken at constant $n/N=1.4 \times 10^{-5}$ concentration of holes in different conjugated polymer-based diodes operated in the space-charge-limited transport regime. An extrapolation of those data to $T \rightarrow \infty$ using Eq. (8) is shown in Fig. 8 by thin curves which intersect at the infinite temperature and yields a $T \rightarrow \infty$ mobility of $\mu_0 \approx 30$ cm²/V s. Thus, no MNR effect emerges in this case.

Another important aspect has been revealed upon considering the calculated T dependences of the charge carrier mobility at *higher temperatures* by using Eqs. (2)–(6) (bold curves in Fig. 8). As one can see from Fig. 8(i) there is a perfect agreement with experimental data which were taken at moderately large temperatures and the calculations corroborate $1/T$ dependence in this temperature range, (ii) at higher temperatures there is a significant deviation of the calculated temperature dependences from Arrhenius' law. This implies unambiguously that extrapolation of $\ln(\mu) \propto T^{-1}$ graphs to $T \rightarrow \infty$ is *illegitimate* as it is illegitimate in the “MNR” case shown in Fig. 1(a). The reason is that at higher temperatures the ODOS is no longer determined by the T -independent carrier concentration but by the T -dependent shift of the ODOS toward the transport energy and, concomitantly, toward the center of the DOS. At high temperatures when ε_0 shifts beyond the Fermi level ε_F , $\mu_e(T)$ approaches the conventional $\ln(\mu) \propto T^{-2}$ dependence^{4,6} (inset in Fig. 8), featuring a $T \rightarrow \infty$ prefactor mobility μ_1 of about 0.16 cm²/V s. This is, indeed, consistent with data derived from ToF studies^{4,6} as well as with the initial mobil-

ity of nonrelaxed charge carriers measured at 1 ps in a conjugated polymer,³⁸ but inconsistent with the conclusion in Ref. 10 predicting unjustifiably large values of ≈ 30 cm²/V s. The latter value seems to be unrealistic for noncrystalline organic materials as the effective mobility in a polymer film is always rate limited by interchain hopping between weakly coupled neighboring polymer chains. Thus, the extrapolation of the Arrhenius $\ln(\mu) \propto T^{-1}$ dependence of the mobility to infinite temperature is at clear variance with the concept of charge hopping transport in organic random systems with a Gaussian-type DOS, that has been also recently discussed by van Mensfoort *et al.*,³³ even though the conventional experimentally accessible temperature range does not allow experimental verification of the predicted change to $\sim T^{-2}$ dependence at a higher temperature. This effect is expected to be also held for a more complex DOS profiles, e.g., a bimodal Gaussian DOS distribution relevant to trap containing materials,^{39,40} as this does not change the basic Gaussian disorder formalism.

In addition to the above discussion it should be mentioned that if the DOS would—hypothetically—be an exponential, the extrapolation suggested in Ref. 10 would be justified. However, we should emphasize that the notion on an exponential DOS strongly contradicts to the results of ToF measurements in the studied polymers,^{41–43} which feature *non-dispersive* photocurrent transients that is an unambiguous evidence for the Gaussian DOS. The point is that in the case of an exponential DOS the ToF transients have to be dispersive as it was demonstrated by Arkhipov *et al.*⁴⁴ because they would never equilibrate during the transit time at small carrier concentrations and should follow Scher-Montroll dispersive transport model.⁴⁵ This is also in accord with work of Mueller-Horsche *et al.*⁴⁶ who measured ToF transients in poly-vinylcarbazole over about seven decades in time and found dispersive transport at short times and saturation at times comparable to the transit time. They analyzed the results by invoking an exponential DOS and found that some cutoff must be introduced to explain occurrence of the equilibration at longer times. These results—including the temperature dependence—can alternatively be well explained in terms of a Gaussian DOS with traps.³⁹ Further, it seems to be improbable that Gaussian DOS at low carrier concentration ($n/N \leq 10^{-7}$) relevant for ToF experiments changes to an exponential one for moderately large concentration ($\approx 10^{-5}$) relevant for the SCL diodes. Change in the DOS shape due to Coulomb interaction is expected at much higher carrier concentration, viz. 10^{-2} , as shown by Zhou *et al.*⁴⁷

The disorder parameter σ can be extracted from the fitting of experimental data (see Table I). The agreement with σ values, determined before from measured temperature dependences of the hole mobility in these materials, is gratifying.

The above consideration implies that for the charge mobility there is in fact no genuine correlation between the prefactor and the Arrhenius factor that arises from activated jumps, i.e., there can be no change in the attempt of the jump frequency, and therefore the *MNR phenomenon in these materials is an apparent rather than true one*. Nonetheless, we show that important material parameters can be derived by analysis of such experimental within the suggested theory.

TABLE I. Material parameters derived from the fitting of the data in Fig. 8.

	E_a (eV)	σ (eV)	σ (eV)	μ_1 (cm ² /V s)
	Experiment	Experiment	Present fitting	Present fitting
BPCM	0.23 ^a	0.075 ^b	0.068	0.16
P3HT	0.32 ^a	0.098 ^c	0.095	0.16
OC ₁ C ₁₁ -PPV	0.48 ^a	0.11–0.12 ^d	0.142	0.16

^aReference 10.

^bReference 48.

^cReference 35.

^dReference 49.

B. Origin of the MNR-type behavior in a Gaussian-type hopping-transport system

The straightforward conclusion is that the apparent observation of MNR is related to charge accumulation in a conductive channel of a OFET at variable gate voltage and has nothing to do with compensation between prefactor and activation energy in a thermally activated kinetic process. Since in the current theory (i) the polaronic character of the charge carrier was ignored, and (ii) the input prefactor in the expression for the jump rate is invariant, the apparent MNR behavior must solely be due to the distribution of the charges within the DOS upon increasing their concentration. The present theory allows to calculate how the shape of the ODOS evolves as a function of charge concentration [Fig. 9(a)]. For very small carrier concentration, $n/N=10^{-7}$, the ODOS is a Gaussian with the same width as that of the DOS itself yet displaced by $\varepsilon_0 = -\sigma^2/k_B T$. Note that the majority of the activated jumps start mostly from upper portion of the ODOS rather than from its center. When the DOS is loaded by charge carriers the shift of the ODOS distribution toward the DOS center is accompanying by *gradual shrinking* (narrowing) with increasing carrier concentration [see inset in Fig. 9(a)]. Therefore, activated jumps start, on average, from somewhat lower (occupied) states implying that the mobility increases less as function of carrier concentration comparing to what one would expect if the ODOS retains its shape. This explains why $\ln \mu_c(T^{-1})$ graphs intersect at finite temperature T_0 at variable n/N while at constant (moderately large) n/N they intersect at $T \rightarrow \infty$.

Figure 9(a) shows how the energetic distribution of charge carriers, migrating within a Gaussian DOS evolves as a function of charge carrier concentration. For $n/N \rightarrow 0$ the ODOS is virtually empty. It is temperature dependent and describes which energy level an individual carrier visits in the course of its stochastic motion. In this case the Fermi level is well below the ODOS center. Upon progressive state filling due to carrier injection into the OFET—the countercharges are located within the gate electrode—Fermi level is being gradually lifting and is located within the ODOS.^{21,35,50} Its leading edge shrinks yet it is still much broader than in a classic semiconductor. This controls charge transport as function of both carrier concentration and temperature.

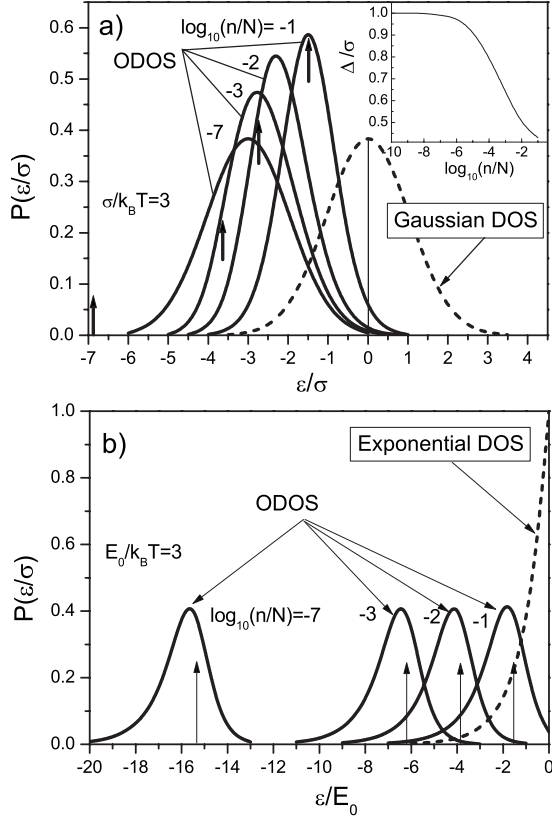


FIG. 9. Normalized ODOS distribution in a disordered organic system with (a) Gaussian DOS and (b) exponential DOS at different carrier concentrations n/N calculated by Eq. (2). The DOS distribution is shown by dotted curve for reference. Arrows indicate position of calculated Fermi levels for the considered carrier concentrations. E_0 is the width of the exponential DOS. Inset in (a) shows calculated width of the ODOS, Δ , as a function of carrier concentration.

Another factor contributing to the MNR behavior is that the maximum of the ODOS distribution ε_m in a disordered organic solid at very high carrier concentrations lifts up somewhat weaker than the Fermi level as it can be seen in Fig. 10. At low carrier concentrations the maximum of

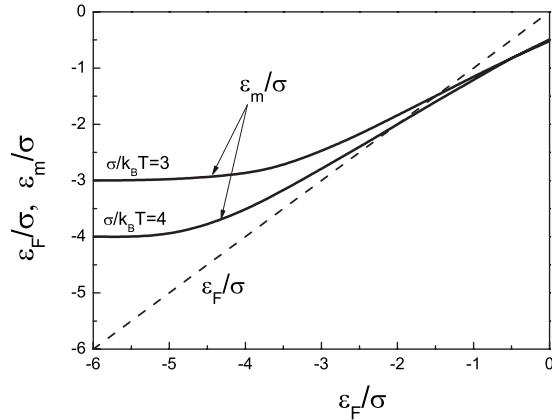


FIG. 10. Maximum of ODOS distribution ε_m in a disordered organic semiconductor as a function of Fermi level ε_F position with respect to the DOS center calculated for two values of $\sigma/k_B T$.

ODOS coincides with the equilibrium level $\varepsilon_m = \varepsilon_0 = -\sigma^2/k_B T$, $\varepsilon_F \ll \varepsilon_m$ and does not depend on carrier concentration or Fermi-level position, as expected. When Fermi level ε_F approaches the ε_0 , the maximum of the ODOS ε_m is also lifting up but its increase appears to be slightly *weaker* than of Fermi level, so eventually they intersect at a certain value of carrier concentration.

We should emphasize that Gaussian-shaped DOS is of key importance for reproducing the MNR behavior in the framework of the suggested model. In the case of exponential DOS, the ODOS distribution, as follows from the calculations [Fig. 9(b)], always retains its shape independent on the carrier concentration. This circumstance has another important implication showing that approximating a Gaussian DOS by an exponential distribution, where thermal quasi-equilibrium level ε_0 is never established⁴⁴ in ToF experiments, is unjustified for organic solids and potentially cannot predict correctly the temperature dependence of the mobility. The detailed study of the impact of different functional dependence of DOS distributions on the above phenomena will be considered elsewhere.

Finally we should discuss the low-temperature branch of the calculated $\mu_e(T)$ dependences described in Sec. II B. Interestingly, that the presented EMA theory predicts a transition to a Mott-type VRH regime at low enough temperatures and large carrier density. The principal reason for this effect is that the effective transport energy level ε_t depends on temperature^{21,28–30} and shifts toward deeper tail states of the DOS with lowering temperature. A Mott-type VRH regime establishes when ε_t becomes close to the Fermi level ε_F . This finding is in accord with recent percolation theory suggested by Zvyagin,³¹ which also conforms a transition from the activated hopping to the Mott-type VRH transport depending on carrier density and temperature. Further, as in the case of the high-temperature branch of $\mu_e(T)$, the presented EMA model predicts dependence of the charge mobility on carrier concentration also in low-temperature Mott-type VRH transport regime, and for both regimes the MNR behavior is recovered with corresponding isokinetic temperatures T_0 and T_1 ($T_0 > T_1$). However, although the presented model is able to describe well the activated hopping transport from high to moderately low temperatures and successfully fits the experimental $\mu(T)$ data for C₆₀-based OFET as well as for other organic semiconductors, the present version of the theory fails to describe quantitatively the observed $\mu(T)$ dependences at very low temperatures.⁵¹ A more advanced EMA theory has to be developed for the low-temperature branch of $\mu_e(T)$ dependences and this issue shall be a subject of our further research.

VI. CONCLUSION

In summary, the principal results of this study are the following: (i) the observed MNR behavior for the OFET charge mobility in organic disordered solids is demonstrated to be a direct consequence of the functional dependence of state filling in a Gaussian-type hopping system and polaron formation might not necessarily be involved to rationalize this phenomenon; (ii) narrowing of the occupational DOS

profile upon increasing carrier concentration occurs for materials with Gaussian DOS distribution (but not for exponential DOS) and gives rise to a MNR effect; (iii) extrapolation of the $\ln(\mu) \propto T^{-1}$ data to $T \rightarrow \infty$ suggested in previous studies¹⁰ is unwarranted and yields unjustifiably large the mobility prefactor; (iv) the MNR effect has been studied in a OFET based on C₆₀ films, a material with very weak electron-phonon coupling, and was successfully described by the present model; (v) the obtained compact analytical relations can be readily used for estimation of important material parameters and effective carrier concentration from experimentally accessible $\mu(T)$ data; (vi) the presented analytical formalism predicts a transition to a Mott-type charge carrier hopping regime at very low temperatures.

ACKNOWLEDGMENTS

The research was implemented within the bilateral ÖAD Project UA-10/2009, and supported by the program of fundamental research of the NAS of Ukraine through the Project No. 10/09-H, and by the Ministry of Education and Science of Ukraine. H.B. acknowledges financial support by the Fond der Chemischen Industrie. The Austrian authors were supported by the NFN under Projects No. S9706 and No. S9711, financed by the Austrian Foundation for Science and Research.

- ¹J. H. Burroughes, D. D. C. Bradley, A. R. Brown, R. N. Marks, K. Mackay, R. H. Friend, P. L. Burns, and A. B. Holmes, *Nature (London)* **347**, 539 (1990).
- ²C. D. Dimitrakopoulos, S. Purushotaman, J. Kymissis, A. Callegari, and J. M. Shaw, *Science* **283**, 822 (1999).
- ³C. J. Brabec, N. S. Sariciftci, and J. C. Hummelen, *Adv. Funct. Mater.* **11**, 15 (2001).
- ⁴H. Bässler, *Phys. Status Solidi B* **175**, 15 (1993).
- ⁵P. W. M. Blom and M. C. J. M. Vissenberg, *Mater. Sci. Eng.* **27**, 53 (2000).
- ⁶V. I. Arkhipov, I. I. Fishchuk, A. Kadashchuk, and H. Bässler, in *Semiconducting Polymers: Chemistry, Physics and Engineering*, 2nd ed., edited by G. Hadziioannou and G. Malliaras (Wiley-VCH Verlag, Weinheim, 2007).
- ⁷I. Zvyagin, in *Charge Transport in Disordered Solids with Applications in Electronics*, edited by S. Baranovski (John Wiley & Sons, Chichester, England, 2006).
- ⁸N. F. Mott and E. A. Davis, *Electronic Processes in Non-Crystalline Materials*, 2nd ed. (Oxford University Press, London, 1979).
- ⁹R. C. G. Naber, C. Tanase, P. W. M. Blom, G. H. Gelinck, A. W. Marsman, F. J. Touwslager, S. Setayesh, and D. M. de Leeuw, *Nature Mater.* **4**, 243 (2005).
- ¹⁰N. I. Craciun, J. Wildeman, and P. W. M. Blom, *Phys. Rev. Lett.* **100**, 056601 (2008).
- ¹¹W. Meyer and H. Neldel, *Z. Tech. Phys. (Leipzig)* **18**, 588 (1937).
- ¹²W. B. Jackson, *Phys. Rev. B* **38**, 3595 (1988).
- ¹³Y. F. Chen and S. F. Huang, *Phys. Rev. B* **44**, 13775 (1991).
- ¹⁴J. C. Wang and Y. F. Chen, *Appl. Phys. Lett.* **73**, 948 (1998).
- ¹⁵P. Stallinga and H. L. Gomes, *Org. Electron.* **6**, 137 (2005).
- ¹⁶R. S. Crandall, *Phys. Rev. B* **43**, 4057 (1991).
- ¹⁷R. Widenhorn, A. Rest, and E. Bodegom, *J. Appl. Phys.* **91**, 6524 (2002).
- ¹⁸A. Yelon and B. Movaghar, *Phys. Rev. Lett.* **65**, 618 (1990).
- ¹⁹D. Emin, *Phys. Rev. Lett.* **100**, 166602 (2008).
- ²⁰I. I. Fishchuk, A. Kadashchuk, H. Bässler, and S. Nešpůrek, *Phys. Rev. B* **67**, 224303 (2003); P. E. Parris, V. M. Kenkre, and D. H. Dunlap, *Phys. Rev. Lett.* **87**, 126601 (2001).
- ²¹I. I. Fishchuk, V. I. Arkhipov, A. Kadashchuk, P. Heremans, and H. Bässler, *Phys. Rev. B* **76**, 045210 (2007).
- ²²A. Devos and M. Lannoo, *Phys. Rev. B* **58**, 8236 (1998).
- ²³E. Frankevich, Y. Maruyama, and H. Ogata, *Chem. Phys. Lett.* **214**, 39 (1993).
- ²⁴Y. Roichman and N. Tessler, *Appl. Phys. Lett.* **80**, 1948 (2002).
- ²⁵E. J. Meijer, E. J. Meijer, M. Matters, P. T. Herwig, D. M. de Leeuw, and T. M. Klapwijk, *Appl. Phys. Lett.* **76**, 3433 (2000).
- ²⁶E. J. Meijer, Ph.D. thesis, Technical University of Delft, 2003.
- ²⁷J. Paloheimo and H. Isotalo, *Synth. Met.* **56**, 3185 (1993).
- ²⁸S. D. Baranovskii, T. Faber, F. Hensel, and P. Thomas, *J. Phys.: Condens. Matter* **9**, 2699 (1997).
- ²⁹A. Kadashchuk, Y. Skryshevskii, A. Vakhnin, N. Ostapenko, V. I. Arkhipov, E. V. Emelianova, and H. Bässler, *Phys. Rev. B* **63**, 115205 (2001).
- ³⁰V. I. Arkhipov, P. Heremans, E. V. Emelianova, G. J. Adriaenssens, and H. Bässler, *J. Phys.: Condens. Matter* **14**, 9899 (2002).
- ³¹I. P. Zvyagin, *Phys. Status Solidi C* **5**, 725 (2008).
- ³²R. Coehoorn, W. F. Pasveer, P. A. Bobbert, and M. A. J. Michels, *Phys. Rev. B* **72**, 155206 (2005).
- ³³S. L. M. van Mensfoort, S. I. E. Vulto, R. A. J. Janssen, and R. Coehoorn, *Phys. Rev. B* **78**, 085208 (2008).
- ³⁴C. Godet, *Philos. Mag. B* **81**, 205 (2001); *J. Non-Cryst. Solids* **299-302**, 333 (2002); *Phys. Status Solidi B* **231**, 499 (2002).
- ³⁵C. Tanase, E. J. Meijer, P. W. M. Blom, and D. M. de Leeuw, *Phys. Rev. Lett.* **91**, 216601 (2003).
- ³⁶N. Kirova and M. N. Bussac, *Phys. Rev. B* **68**, 235312 (2003).
- ³⁷H. Houili, J. D. Picon, and L. Zuppiroli, *J. Appl. Phys.* **100**, 023702 (2006); I. N. Hulea, S. Fratini, H. Xie, C. L. Mulder, N. N. Oossad, G. Rastelli, S. Ciuchi, and A. F. Morpurgo, *Nature Mater.* **5**, 982 (2006).
- ³⁸A. Devižis, A. Serbenta, K. Meerholz, D. Hertel, and V. Gulbinas, *Phys. Rev. Lett.* **103**, 027404 (2009).
- ³⁹U. Wolf, H. Bässler, P. M. Borsenberger, and W. T. Gruenbaum, *Chem. Phys.* **222**, 259 (1997).
- ⁴⁰I. I. Fishchuk, A. K. Kadashchuk, H. Bässler, and D. S. Weiss, *Phys. Rev. B* **66**, 205208 (2002); I. I. Fishchuk, A. K. Kadashchuk, A. Vakhnin, Yu. Korosko, H. H. Bässler, B. Souharce, and U. Scherf, *ibid.* **73**, 115210 (2006).
- ⁴¹A. J. Mozer and N. S. Sariciftci, *Chem. Phys. Lett.* **389**, 438 (2004); A. J. Mozer, N. S. Sariciftci, A. Pivrikas, R. Österbacka, G. Juška, L. Brassat, and H. Bässler, *Phys. Rev. B* **71**, 035214 (2005).

- ⁴²A. R. Inigo, C. C. Chang, W. Fann, J. D. White, Y.-S. Huang, U.-S. Jeng, H. S. Sheu, K.-Y. Peng, and S.-A. Chen, *Adv. Mater. (Weinheim, Ger.)* **17**, 1835 (2005).
- ⁴³R. U. A. Khan, D. Poplavskyy, T. Kreouzis, and D. D. C. Bradley, *Phys. Rev. B* **75**, 035215 (2007).
- ⁴⁴V. I. Arkhipov, A. I. Rudenko, M. S. Iovu, and S. D. Shutov, *Phys. Status Solidi A* **54**, 67 (1979).
- ⁴⁵H. Scher and E. W. Montroll, *Phys. Rev. B* **12**, 2455 (1975).
- ⁴⁶E. Müller-Horsche, D. Haarer, and H. Scher, *Phys. Rev. B* **35**, 1273 (1987).
- ⁴⁷J. Zhou, Y. C. Zhou, J. M. Zhao, C. Q. Wu, X. M. Ding, and X. Y. Hou, *Phys. Rev. B* **75**, 153201 (2007).
- ⁴⁸V. D. Mihailetchi, J. K. J. van Duren, P. W. M. Blom, J. C. Hummelen, R. A. J. Janssen, J. M. Kroon, M. T. Rispens, W. J. H. Verhees, and M. M. Wienk, *Adv. Funct. Mater.* **13**, 43 (2003).
- ⁴⁹H. C. F. Martens, P. W. M. Blom, and H. F. M. Schoo, *Phys. Rev. B* **61**, 7489 (2000).
- ⁵⁰W. F. Pasveer, J. Cottaar, C. Tanase, R. Coehoorn, P. A. Bobbert, P. W. M. Blom, D. M. de Leeuw, and M. A. J. Michels, *Phys. Rev. Lett.* **94**, 206601 (2005).
- ⁵¹Mujeeb Ullah, T. B. Singh, H. Sitter, and N. S. Sariciftci, *Appl. Phys. A* **97**, 521 (2009).